Seasonal Variation and Heat Preference of the South Asia High

Qian Yongfu (钱永甫),[1①] Zhang Qiong (张 琼),[2] P4 A
Yao Yonghong (姚永红),[1] and Zhang Xuehong (张学洪)[2]

[1]*Department of Atmospheric Sciences, Nanjing University, Nanjing* 210093
[2]*LASG, Institute of Atmospheric Physics, Chinese Academy of Sciences, Beijing* 100029

(Received August 21, 2001; revised May 10, 2002)

ABSTRACT

By use of the NCEP / NCAR reanalysis data, the seasonal variation of the South Asia high (SAH) is analyzed. The influences of temporal and spatial variations of the middle and upper level atmospheric temperatures, the visible heat sources, and the diabatic heating rates in the whole atmospheric column on the seasonal variation of the SAH are discussed. Results show that the SAH has two seasonal balancing modes, one of which is the land high in summer and the other the ocean high in winter. The land high itself can be divided into two patterns as well, that is the Tibetan high and the Iranian high. Heating fields have important impacts on the seasonal variation of the SAH. The SAH is a warm high and its center has the property of heat preference, usually locating over or moving to an area with relatively larger heating rates. The annual cycle of the SAH is mainly controlled by the seasonal process of the latent and sensible heating in South Asia. Strong shortwave radiative heating in the north at high latitudes and over the Tibetan Plateau also has an effects on the northward movement and maintenance of the SAH. The cooling effect of infrared radiation is an important cause in weakening the SAH.

Key words: the South Asia high, seasonal balancing modes, seasonal variation, heating fields, mechanism study

1. Introduction

Each summer, there is one lower stratosphere semi-permanent anticyclonic circulation over the Tibetan Plateau (TP) called "the Tibetan high", which is the strongest near the 100 hPa level. The High's center at the 100 hPa level is also frequently located over the Iranian Plateau (IP). In winter, there is an anticyclonic circulation over the ocean, moving northwestward gradually with the change of season and forming a high center. By summer, the circulation reaches the TP and the IP, completing an annual cycle. Therefore, we define both of the winter anticyclonic circulation over ocean and the summer one over land as the South Asia high (SAH) in this paper.

There are many studies on the SAH. Mason and Anderson (1958) pointed out, that, according to the data collected in the International Geophysical Year, the SAH is the strongest, largest, and most stable anticyclonic circulation system at the 100 hPa level in the Northern Hemisphere. Flohn (1960) indicated that the SAH results from the heating effect of the TP. Tao and Zhu (1964) studied the impacts of the SAH on circulation in the Northern Hemisphere and the weather and climate in China. In the 1970s, meteorologists in China widely

①E-mail: qianzh2@netra.nju.edu.cn

studied the climatic features, the patterns of activities, the formation mechanisms, and the relationship with precipitation in various regions of China. The activities of the SAH became an important basis for weather prediction in the rainy season (see Sun and Song 1987; Luo et al. 1982; Krishnamurti et al. 1973; Zhang and Peng 1983; Zhou 1991). However, many of the past studies were case analyses of the SAH and its synoptic processes due to the lack of data, research methodology, and computation ability. In recent years, the authors used the newer and longer global NCEP/NCAR reanalysis data set to reanalyze the climatological properties of interannual, decadal, and interdecadal variations and the relationships to the ENSO events of the SAH. It is found that the SAH is also a strong signal of climate change in the atmosphere (see Zhang et al. 2000).

It is well known that the seasonal variation is the basis of interannual, decadal, and interdecadal variations. If there were no abnormality in the seasonal variation, there would be no interannual, decadal, or interdecadal variations. Zhu et al. (1980) proved that the SAH has obvious seasonal variation. As to the cause of the seasonal variation, Sun (1984) emphasized the heating effect of the TP and the ocean–land thermal contrast. Liu et al. (2000) stressed the importance of the so–called baroclinic circulation. Zhang (1977) pointed out that the formation of the SAH is mainly induced by thermal effects, while its movement in large domains results from circulation adjustment. Qian (1978) found that the heating field is a pretty fair predictive indication of circulation evolution. Therefore, most researchers emphasized the thermal effect of the heating field on the SAH formation. However, it is still necessary to further study the seasonal properties and the mechanisms of the SAH deeply in order to discuss the physical causes of its interannual and interdecadal variations more thoroughly.

2. Data, research domain, and definitions of the SAH characteristic parameters

The data used are the NCEP/NCAR reanalysis data from January 1958 to May 1998 including monthly mean velocity, geopotential height, and temperature fields at various isobaric surfaces. In order to analyze the cause inducing the seasonal variation of the SAH, the monthly mean heat fluxes, radiation fluxes, and monthly precipitation fields in all months of the 15 years from 1980 to 1994 are also utilized. All data is on a $2.5^\circ \times 2.5^\circ$ latitude–longitude grid.

The research domain is determined on the basis of analyzing the geopotential height and circulation patterns at the 100 hPa level in various months of the 40 years from January 1958 to May 1998. It is located in 30°W–180°E, 53°S–55°N in order to contain all the activity areas of the SAH in both summer and winter.

The line along which the u–component of wind is equal to zero is defined as the ridgeline of the SAH. Moreover, to the north of the ridgeline, $u > 0$, and to south, $u < 0$. The ridgeline crosses different meridians at different latitudes and may break at some meridians, so the average of latitudes at different meridians is taken as the mean ridgeline of the SAH. The center of the SAH is defined at the point with the largest geopotential height and is expressed by its longitude and latitude.

The area of the SAH is computed by counting the points at which the geopotential height should be equal to or greater than the characteristic height of 1660 gpdm. Therefore, the area is expressed as the number of total points counted and designated with A_s.

Three kinds of the SAH intensity are defined, the center intensity I_1 which is the geopotential height at the center, the absolute intensity I_2 which is the sum of differences between the geopotential height at each point and the characteristic one in the SAH area,

and the mean intensity I_3 which is the ratio between I_2 and A_s.

3. Seasonal variation of the SAH

3.1 *Seasonal variations of the SAH characteristic parameters*

Figure 1a shows the seasonal variations of the 40-year average SAH center (solid line) and mean ridgeline latitude (dotted line). The variations of the two parameters are basically the same with the only difference as the latter being shifted a little southward. The center and the ridgeline are both located in tropical regions south of 15°N before April. They jump abruptly northward to the north of 20°N in May, move northward largely again in June with the former near 30°N, reach to the northern-most positions north of 30°N in July and August, retreat southward continuously after September, and return to tropical regions by December.

Figure 1b is the same as Fig. 1a but for the SAH center longitude. It is seen that there are two evident sudden changes, one in spring (February to April) and the other in autumn (September to November). In spring, the SAH advances westward suddenly to the Indo-China Peninsula (ICP) from the ocean, and in autumn, it retreats eastward rapidly. Combined with

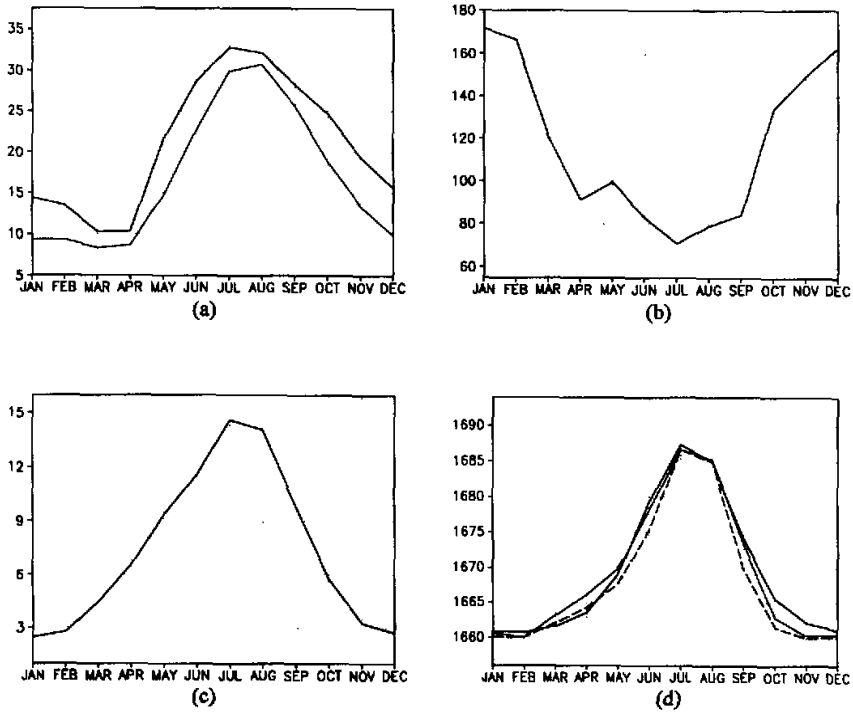

Fig. 1. Seasonal variations of the 40 years average SAH parameters. (a) Latitudes of center and mean ridgeline, (b) center longitude, (c) area (unit: 100) and (d) three intensities.

the time variation of the center latitude, it is found that the SAH center remains in the tropical region when advancing in spring, while it retreats southeastward from the TP along a different path when withdrawing in autumn.

The SAH area A_s has evident seasonal variation, too, as shown in Fig. 1c. The area is the smallest in winter, increases gradually after, and reaches a maximum in July and August.

The three intensities of the SAH have very similar seasonal variations (see Fig. 1d). In order to plot all the three intensities in one diagram, I_2 and I_3 are both transformed by the formula:

$$I' = 1660 + [I - I(m)][I_1(M) - I_1(m)] / [I(M) - I(m)] ,$$

where M and m denote the maximum and minimum of intensity, respectively, and I represents I_2 or I_3. It is seen from Fig. 1d that the seasonal variations of the intensities are fairly consistent with that of the area A_s. From Fig. 1a–1d it is also found that the northwestward advance of the SAH center is more abrupt than its southeastward withdrawal, while the area and the intensities of the SAH change more rapidly during their southeastward withdrawal.

3.2 *The two balancing modes of the SAH parameters in seasonal cycling*

There is an obvious interannual difference in the seasonal variations of the SAH. Anomalies in various months with both annual and interannual variations can be obtained by subtracting the average of the 480 monthly mean parameters of the 40 years from the corresponding monthly mean one. Figure 2 gives the seasonal and interannual variations of various characteristic parameters of the SAH with the ordinate denoting years and the abscissa months.

It is seen from Fig. 2 that the seasonal transition of the SAH mean ridgeline happens in May and in Octoper–November with weaker interannual and interdecadal variations (Fig. 2a). The seasonal transition of the center longitude appears in February–April and in October with apparent interannual variation from winter to summer (Fig. 2b). Large interannual and interdecadal variations are found in the seasonal transition of the area. Before 1978, the winter to summer transition is in February–June while after 1978, it is in February–April, ending about two months in advance. Moreover, the anomalies in summer (JJA) are much bigger than those before 1978. Large interannual and interdecadal variations are also found in the summer to winter transition. Before 1978, the transition is in September and after 1978, it is in October–November with a one– or two–month delay (Fig. 2c). The intensity transition has similar features (Fig. 2d). It is inferred that the seasonal and interannual anomalies of the center longitude, the area, and the intensity of the SAH may have a more evident climatic impacts. For example, they may have a close relationship with the El Niño event as shown in Fig.2. In El Niño years larger positive anomalies of the SAH area and intensity occur, the seasonal transition of the center longitude is earlier, and the position shifts more westward.

Figure 2 shows the close relationship between the interannual and the seasonal variations as well. Taking the SAH intensity as an example (Fig. 2d), the SAH is more intense in the summers of 1980, 1983, 1988, and 1991. The seasonal transitions of intensity are all earlier in those years, too. While in 1975, 1981, 1985, 1989, and 1992, the seasonal transitions are all later and the intensities of the SAH weaker. Similar situations exist for other parameters. Therefore, the seasonal anomaly is indeed the basis for the interannual variation.

Figure 3 shows (a) the frequency and (b) the geographic distributions of the SAH center with longitude. It is seen from Fig. 3a that there are two balancing modes of the SAH along

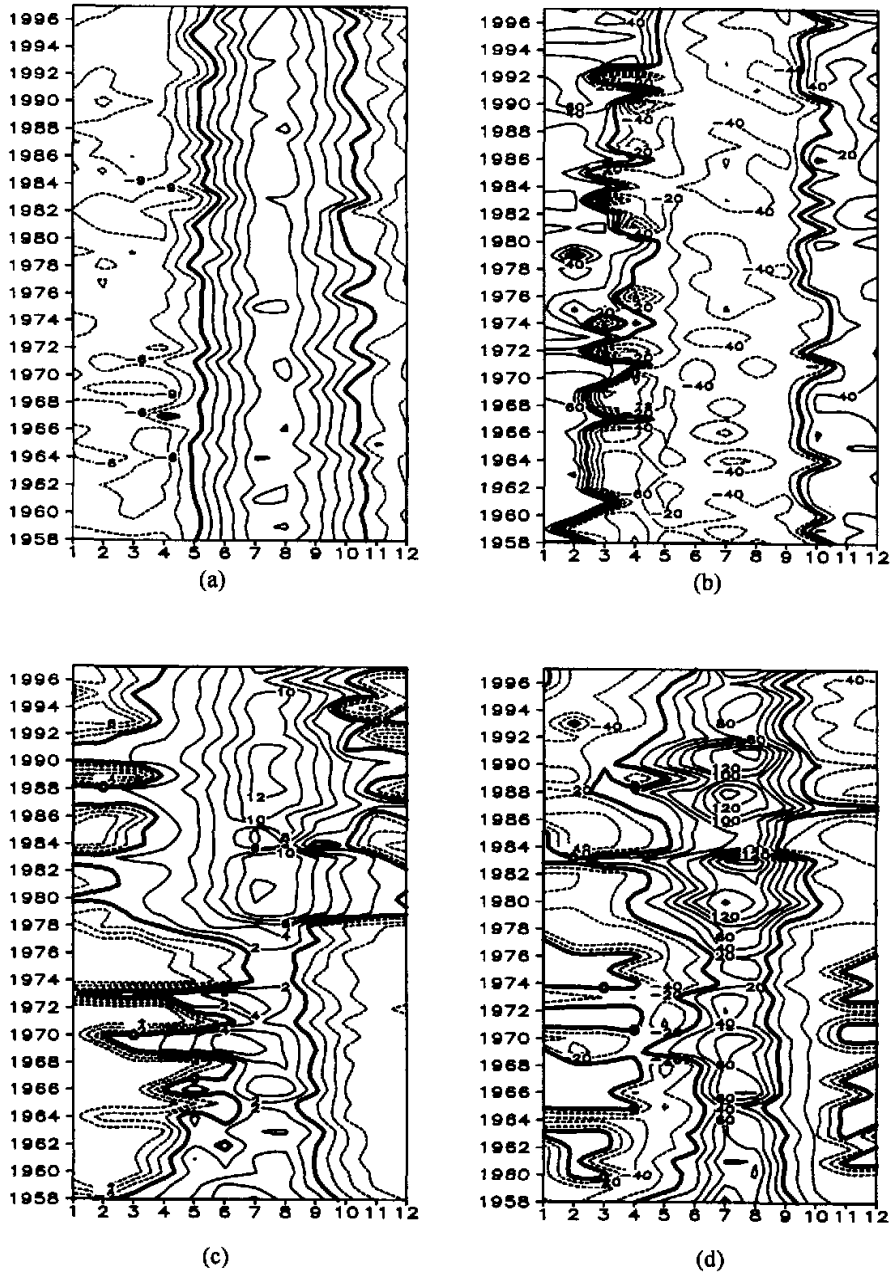

Fig. 2. Seasonal and interannual variations of the SAH characteristic parameters. (a) Mean ridgeline latitude, (b) center longitude, (c) area, and (d) intensity (I_2).

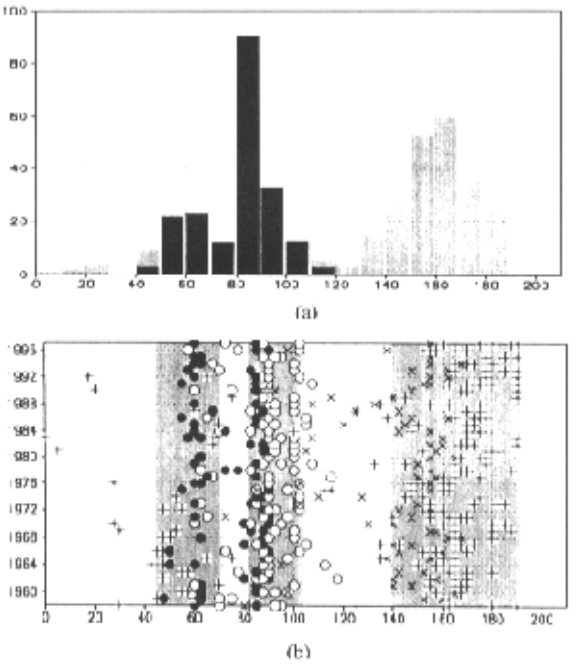

Fig. 3. Frequency (a) and geographic (b) distributions of the SAH center with longitude. Symbol "+" represents the SAH center position in December to April, "○" in May, June and September, "●" in July and August of mid summer, "×" in October and November.

longitude. In winter, the SAH centers are usually located over ocean (lightly shaded) while in summer over land (deeply shaded). The summer mode can be divided into two sub-modes with one over the IP in 50°–70°E called "the IH" and the other over the TP in 80°–100°E called "the TH". In China, some meteorologists used to call the two sub-modes the west pattern and the east pattern of the TH. However, they have different thermal structures (see Zhang 1999). From Fig. 3b, it is found that the SAH prefers to stay over the TP in May, June, and September (designated with "○"), over the west TP and the east IP in July and August in mid summer (with "●"), over the Pacific Ocean between 140°E and 170°W in winter from December to April (with "+"), while over the western Pacific between 140°E and 160°E in October and November, the transition season from autumn to winter (with "×").

Zhu et al. (1980) has pointed out that the SAH in summer scarcely appears over 100°E. However, this is not the case in Fig. 3. In fact, the frequency of the SAH along 100°E is not small. The discrepancy may be caused by the short-range data used by Zhu et al..

4. Mechanisms of the SAH seasonal variation

4.1 *Seasonal variation of the temperature field in the mid and upper troposphere*

The change of temperature is the basis of the geopotential height because of the good hydrostatic relationship between them. Therefore, the impacting factors of the SAH seasonal variation can be found by analyzing the causes of the seasonal variation of temperature. Thus, the monthly mean temperature in the mid and upper troposphere is computed by averaging the temperature vertically from the 500 hPa to 100 hPa levels. The characteristic parameters of the mean temperature, such as the positions of warm centers (longitudes and latitudes) and the intensity (temperature values), can be easily determined. The features of the seasonal variations of temperature can be discussed by those parameters as well.

By analyzing the positions and intensities in January to December, it is found that the warm center of the mean temperature in the mid and upper troposphere moves gradually with season from winter to summer from the southeast to the northwest with an increasing center temperature. It reaches the western-most and northern-most position with a maximum temperature value in the mid summer of July and August. There are the same two abrupt seasonal changes in temperature for the SAH in spring and autumn, respectively (figures omitted).

Figure 4 shows (a) the frequency and (b) the geographic distributions of the warm temperature center with longitude. It is indicated in Fig. 4a that from May to September, the warm temperature centers are concentrated over the TP area between 70°E and 110°E (deeply shaded). While from October to the next April, the warm centers are distributed to the east of 120°E and concentrated between 160°E and 170°W (lightly shaded). Compared with Fig. 3a, the frequency distributes more concentrically than the SAH center. The main frequency area in winter of the SAH center is located to the west of that of the warm center, while they are overlapped with each other in summer. Furthermore, the warm centers do not usually appear over the IP. Hence, the IH is a high-pressure system with more dynamic properties. In Fig. 4b, it is depicted that the warm centers in the early summer of May to June and in the early autumn of September are located over the area between 90°E and 105°E (designated with "○"), between 80°E and 90°E in the mid summer of July and August (with "●"), between 130°E and 155°E in October and November (with "×"), and over the ocean to the east of 140°E in December to April (with "+"). Therefore, the warm centers jump suddenly from the oceanic surface east of 150°E to the TP west of 105°E without gradual westward movement, indicating the warm centers over the TP are formed locally in the process of seasonal transition from winter to summer. However, from summer to winter, the warm centers withdraw out of the TP at first, then gradually retreat eastward and settle stably over the tropical central Pacific by mid winter. The case is similar to the seasonal transition of the SAH center (see Fig. 3b).

From the above discussions it can be concluded that the seasonal transitions of the SAH and the warm centers are basically the same. Therefore, the causes of seasonal transition of the SAH may be depicted through the causes of the latter.

4.2 *Impacts of the visible heat source on the SAH seasonal variation*

The seasonal transition of the atmospheric temperature is basically controlled by the atmospheric heating field. Due to the basic consistency of the seasonal transitions between the SAH and the warm center as depicted in the previous paragraph, it is possibly reasonable to

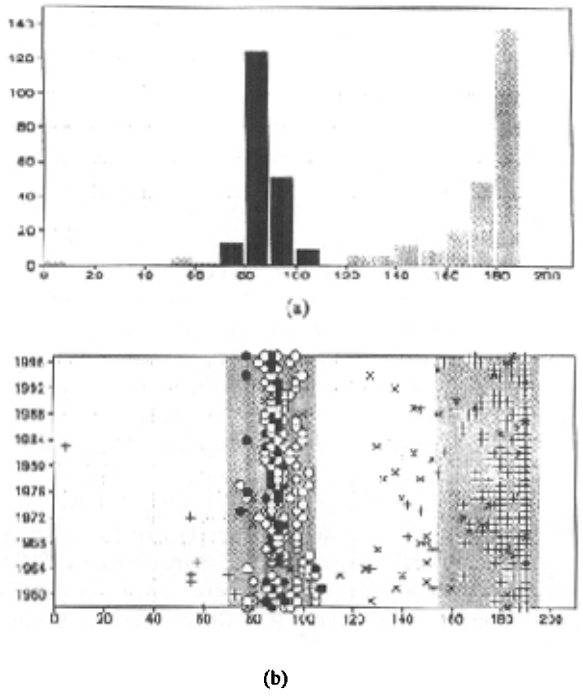

Fig. 4. Frequency (a) and longitudinal (b) distributions of the monthly mean warm centers of the mid–upper troposphere temperature during Jan., 1958 to May, 1998. Others are the same as in Fig. 3.

connect the seasonal transition of the SAH with that of the heating field. The atmospheric heating field can be computed through the thermodynamic equation or the observed heat fluxes. The so–called visible heat source is calculated by use of the former containing only the total value, the local temperature change, the horizontal and vertical advection of heat, and the turbulent exchange, while the computation scheme by use of the observed heat fluxes distinguishes various heating components such as latent, sensible, and radiative heating rates (hereafter abbreviated to " diabatic heating"). The relations between the SAH and the visible heat source are discussed first in this sub–section and then the influences of the diabatic heating on the SAH will be studied. Because the global diabatic heating components we owned are available only during the 15 years from 1980 to 1994, the visible heat source is also computed in the same limited period in order to make the comparison. Besides, the turbulent heat term in the visible heat source cannot be computed using the monthly mean fields, and the accuracy of the computed heat source is influenced to some extent. The heating fields are all transferred to heating rates (K d^{-1}). The Lagrange viewpoint is used in the analysis; that is, the temporal variations of heating rates along the latitude or longitude of the SAH center are studied. In order to explore the effect mechanisms of the heating rates in a total vertical air column on the SAH movements, the mass–weighted averages of the heating rates are calculated in the whole column from the surface to the 100 hPa level.

Figure 5 gives the time–latitude profiles of the latitudinal departures of (a) the local temperature change, (b) horizontal advection, (c) vertical advection, and (d) the total heating rate. Here the latitudinal departure means the difference between a quantity and its latitudinal mean along a meridian. The relative intensity of departures can be used to analyze the cause of the SAH north–south movement. The latitude position of the SAH is shown in Fig. 5 with a rough solid line. The longitude can be found in Fig. 6. Due to the large interannual variation of the SAH (see Zhang et al. 2000) the multi–yearly averaged monthly mean positions of the SAH during the 15 years are somewhat different from those during the 40 years shown in Fig. 1.

It is seen from Fig. 5a that the SAH center moves continuously northward before July, attracted by the relatively large–valued area of local temperature increase at the same longitude. In July it crosses 30°N, reaching its northern–most position, and settles in the relatively small–valued area. After that the SAH center begins to withdraw southeastward and its intensity decreases continuously. No matter whether the SAH center is located in the large–valued area or in the small–valued one, the center always advances or retreats along the gradient of the local temperature increase. Therefore, the meridional difference of the heating effect in the total air column below the 100 hPa level plays an important role in the north–south seasonal transition of the SAH. Figure 5b indicates the influence of horizontal temperature advection on the SAH movement. It is seen that the SAH center is located basically in the cold advection area that weakens the SAH intensity. In order to keep its intensity, the SAH must move to the warm advection area. Thus, the SAH center advances or retreats along the gradient of temperature increase induced by the advection term. Figure 5c points out that the consumption of visible heat is mainly for the maintenance of vertical motion and vertical heat transportation. The SAH center is nearly located in the relatively small–valued area of the two heating rates, indicating strong updrafts in the atmosphere below the SAH. The heat consumed by the strong updrafts must be compensated by the total visible heat source. It is seen from Fig. 5d that the SAH center is located year–round in the relatively large–valued areas of the visible heat source. Before April, the heating rate to south of the SAH center is relatively large, attracting the center to move slightly southward. In May to July, the SAH center advances northward, attracted by the large heating area north of it, and then withdraws southward due to the high heating south of it.

The westward and eastward movements of the SAH center can be explained as above. Figure 6 indicates the time–longitude profiles of the longitudinal departures of (a) the local temperature change, (b) horizontal advection, (c) vertical advection, and (d) the total heating rate. Here the longitudinal departure is the difference between a quantity and its longitudinal mean along a certain latitude. The relative intensity of departure can be used to judge the cause of the SAH east–west movement. The longitude position of the SAH is shown in Fig. 6 with a rough solid line. The latitude can be found in Fig. 5.

It is found that before July the SAH center always moves towards the large–valued area of the local temperature change when it advances continuously westward before July (Fig. 6a). Below the center there are the relatively large cold advection area (Fig. 6b) and the strong upward motion (Fig. 6c). The center is located in the relatively large area of the total visible heating rate and basically moves westward along its gradient (Fig. 6d). After July, the SAH center sits in the relatively small–valued area of the local temperature change, withdrawing eastward along the gradient as well (Fig. 6a), which is consistent with Fig. 5a.

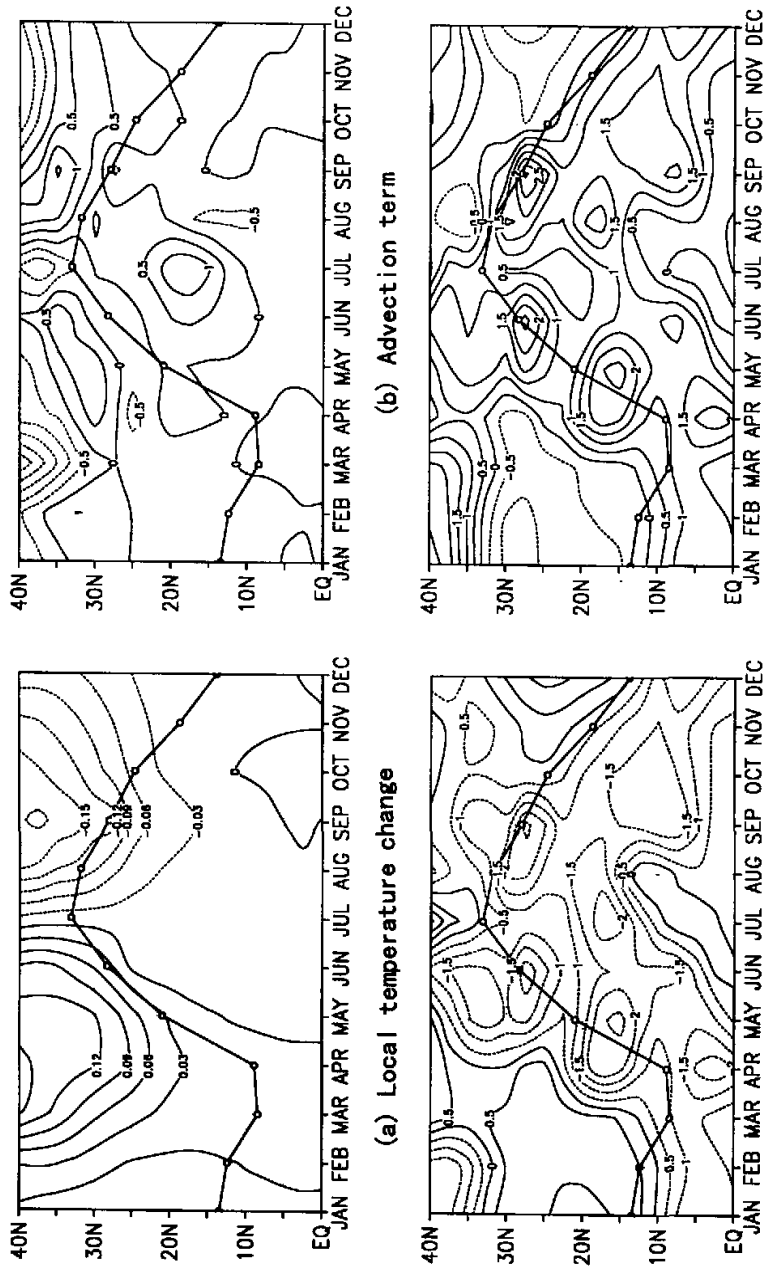

Fig. 5. Time–latitude profiles of the latitudinal departures of the local temperature change (a), horizontal (b) and vertical (c) advection and the total heating rate (d). The latitude position of the SAH is shown with a rough solid line.

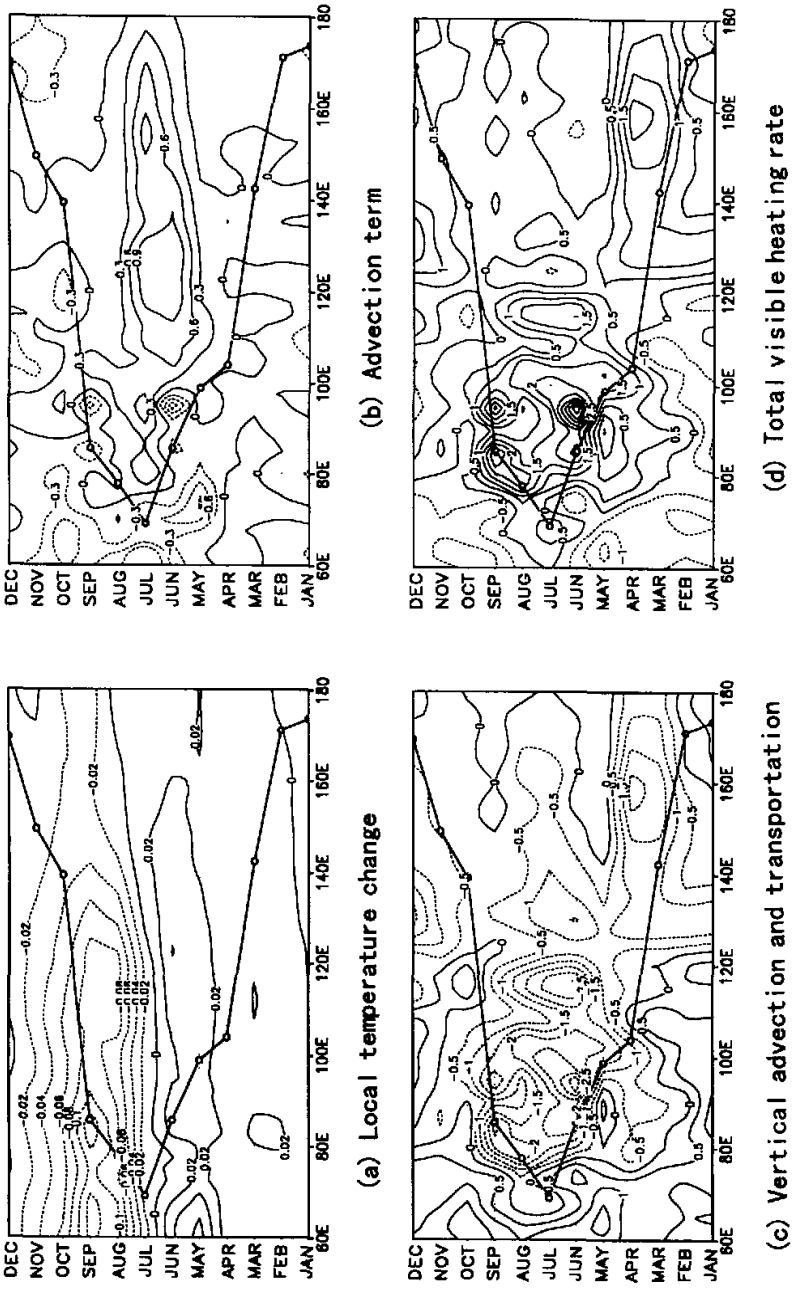

Fig. 6. Time–longitude profiles of the longitudinal departures of local temperature change (a), horizontal (b) and vertical (c) advection and total heating rate (d). The longitude position of the SAH is shown with a rough solid line.

The combined analysis of Figs. 5 and 6 indicates that the SAH center always moves to the relatively large-valued areas of the latitudinal and longitudinal departures of the visible heating rates in its movement, and slows down near the large-valued areas, forming the winter and summer balancing states. Hence, it may be concluded that the SAH has an obvious heat preference.

4.3 *Relationships between diabatic heating and the SAH seasonal variation*

The total diabatic heat flux in an air column from the surface to the top of the atmosphere can be calculated by using the formula

$$Q_{\text{Total}} = Q_s + (F_s^{\uparrow} - F_d^{\downarrow} - F_u^{\uparrow}) + (S_0\overline{\cos Z} - S_d^{\downarrow} + 0.2\times S_u^{\uparrow}) + Q_l + Q_t \ ,$$

where Q_{Total} is the total diabatic heating flux, Q_s the sensible heat flux from the surface, $F_s^{\uparrow}$ the upward longwave radiation flux at the surface, $F_d^{\downarrow}$ the downward longwave radiation flux from the atmosphere near the surface, $F_u^{\uparrow}$ the outgoing longwave radiation flux (OLR), $S_d^{\downarrow}$ the solar radiation flux reaching the surface, $S_u^{\uparrow}$ the shortwave radiation flux leaving the surface, Q_l the latent heat flux released in the atmosphere and estimated with monthly precipitation, and Q_t the turbulent heat flux, which is omitted due to lack of data. Other designations are conventional. The value 0.2 is the mean absorption coefficient of the atmosphere. All diabatic heat fluxes are taken from the NCEP/NCAR monthly mean reanalysis data and treated in the same way as the visible heat source to get the mean atmospheric heating rate in a vertical air column.

Figure 7 shows the time–latitude profiles of the latitudinal departures of heating rates of (a) latent heat, (b) sensible heat, (c) longwave radiation, (d) shortwave radiation, and (e) total diabatic heat fluxes in the SAH center. It is seen from Fig. 7a that the SAH is always located in the relatively large-valued areas of the latent heating in March to September. From April to July, two latent heating centers in 10°–20°N and 25°–35°N make extremely large contributions to the northward movement and intensification of the SAH center. The sensible heating also attracts the SAH center to move northward and intensifies the center. Before September, the sensible heating north of the SAH is very strong all the time, resulting in the maintenance of the SAH in high latitudes (Fig. 7b). The longwave radiation has a cooling effect on the SAH, especially in June to September, inducing the weakening of the SAH (Fig. 7c). The effect of the shortwave radiation is similar to the sensible heating, beneficial to the northward movement and maintenance of the SAH center (Fig. 7d). The time variation of the total heating rate (Fig. 7e) is mainly due to the latent and sensible heating rates (Fig. 7a, b). Before September, the SAH center is always located in the relatively large-valued areas of the total heating, which is the fundamental cause of its northward advance and maintenance. After October, the center sits in the low-valued areas to the north of the large-valued ones of the heating rates located in 5°–15°N, and rapidly withdraws southward due to the attraction of the large heating.

Figure 8 is the same as Fig. 7 but for time–longitude profiles of longitudinal departures. It is seen that all heating components except the longwave radiation positively contribute to the westward movement in April to July and maintenance in 70°–100°E in April to September of the SAH center. After October, the center drops into the relatively small-valued areas and is attracted by the large heating areas appearing in 120°–160°E of the latent and total heat fluxes; it begins to withdraw eastward, weakening at the same time. Comparing Fig. 8e with

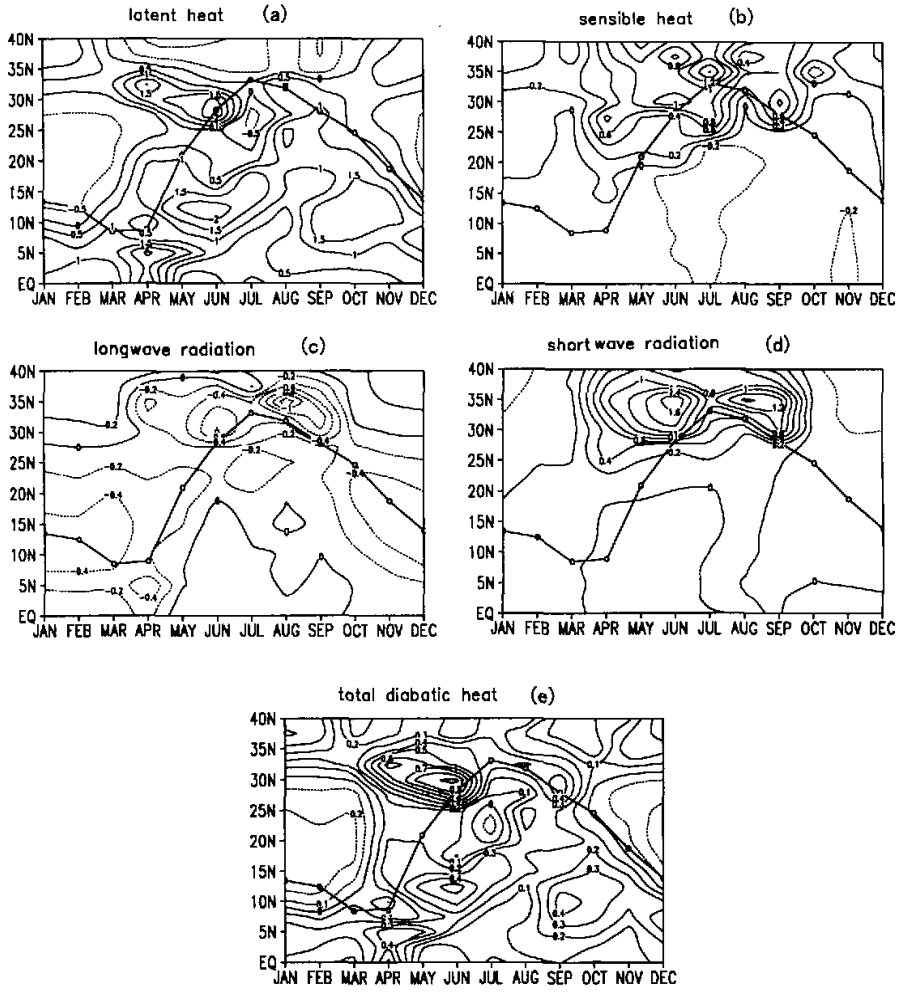

Fig. 7. The time–latitude profiles of latitudinal departures of heating rates of latent heat (a), sensible heat (b), long wave radiation (c), short wave radiation (d), and total diabatic heat (e) fluxes in the SAH center.

Figs. 8a and b, it is found that the total heating rate is again mainly determined by the latent and sensible heat fluxes, especially the latent heating in the tropical regions in April to May in 80°–120°E and the sensible heating over the TP and the IP in 60°–100°E in April to September. The obviously large-valued area of the shortwave radiative heating rate over the TP and the IP also has a non-negligible contribution to the total heating in May to September.

The combined analysis of Figs. 7e and 8e indicates that the SAH center is always attracted by the relatively large-valued areas of the longitudinal and latitudinal departures of

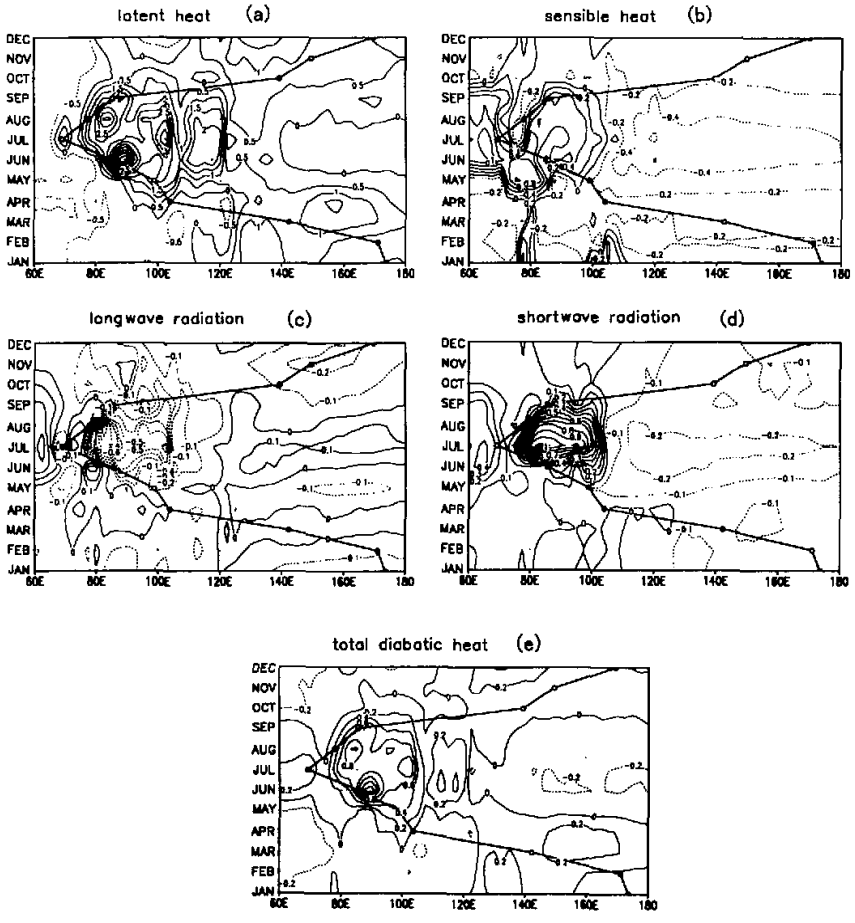

Fig. 8. Time–longitude profiles of longitudinal departures of heating rates of latent heat (a), sensible heat (b), long wave radiation (c), short wave radiation (d), and total diabatic heat (e) fluxes in SAH center.

the total diabatic heating rate, moving towards the areas and forming its seasonal balancing state. For example, in April, the center jumps rapidly from the ocean to the tropical region near 10°N, south of the TP because of the appearance of large–valued areas of the total heating rate in March between the equator and 5°N at 100°E. It abruptly jumps to 20°N from 10°N at 100°E in May due to the existence of large–valued areas of heating between 10°N and 20°N and between 25°N and 35°N at that longitude, with the latter region being greater than the former. The center advances westward to 90°E at 28°N in June, owing to the appearance of the maximum heating rate there. The southward withdrawal and eastward re-

treat of the center after October occurs because a large-valued area of heating forms between 5°N and 15°N in 80°–100°E in September and moves gradually eastward to the east of 120°E. The SAH center follows the large-valued area and returns to the ocean at last. Therefore, the SAH center always moves towards the large-valued areas of heating and thus it has a "heat preference". All the above conclusions are entirely the same as those described in the previous section regarding the visible heat source.

5. Conclusions

From the above discussions it is concluded that the SAH has evident seasonal variation with two seasonal balancing modes, one the summertime land high and the other, the wintertime ocean high. The summertime land high can be divided again into two patterns according to the positions of the center, that is the Tibetan high (TH) and the Iranian High (IH). In the past, the latter was known as the west pattern of the former. The SAH is a warm high and well matches the warm center of temperature averaged in the upper and middle troposphere from the 500 hPa to the 100 hPa level.

It is depicted from the analyses of the temporal and spatial variations of the longitudinal and latitudinal departures of the visible heat source and the sensible, latent, longwave and shortwave radiative and total diabatic heat fluxes that the SAH forms mainly due to the thermal effect of diabatic heating. Its center always moves towards the relatively large-valued areas of the heating rates and thus has a "heat preference". Its movement from the ocean in the winter westward to the Asian continent in the summer and then moving northward, its maintenance over the TP and the IP areas in mid summer, and retreat from the Plateaus and return to the ocean are all mainly controlled by the latent and sensible heating rates in South Asia. The summertime strong shortwave radiative heating in the north and over the TP and the IP also contributes to the northward movement and maintenance of the SAH center, while the longwave radiative cooling in the SAH domain after September is an important factor in weakening the high.

The points obtained above are useful for studies on the mechanisms of interannual and interdecadal variations of the SAH parameters and their relationships with the abnormal changes of climate.

Acknowledgments. This research was jointly sponsored by "The National Key Programme for Developing Basic Sciences" project (1998040900): Part I, and the National Natural Science Foundation of China Project: "Studies on Interaction between the South Asia High and the Asian Monsoon and Its Mechanisms" under Grant No.40175021.

REFERENCES

Flohn, H., 1960: Recent investigation on the mechanism of the 'summer monsoon' of southern and eastern Asia. *Proc. Symp. Monsoon of the World*, New Delhi, Hind Union Press, 75–88.

Krishnamurti, T. N., S. M. Daggupaty, Jay Fein, Masao Kanamitsu, and John D. Lee, 1973: Tibetan high and upper tropospheric tropical circulations during northern summer. *Bull. Amer. Meteor. Soc.*, **54**, 1234–1249.

Liu Xuanfei, Zhu Qiangen, and Guo Pinwen, 2000: Conversion characteristics between barotropic and baroclinic circulations of the SAH and its seasonal evolution. *Advances in Atmospheric Sciences*, **17**(1), 129–139.

Luo Siwei, Qian Zhengan, and Wang Qianqian, 1982: Synoptic and climatic studies on relationships between the Tibetan high and the summer floods and droughts in East China. *Plateau Meteorology*, **1**(2), 1–10 (in Chinese).

Mason, R. B., and C. E. Anderson, 1958: The development and decay of the 100 mb summertime anticyclone over southern Asia. *Mon. Wea. Rev.*, **91**, 3–12.

Qian Yongfu, 1978: Computational scheme of heating fields and their effect on a process of the Tibetan High. *Papers on the Tibetan Plateau Meteorology (1975-1976)*, Science Press, Beijing, 199–212 (in Chinese).

Sun Guowu, 1984: Study on seasonal variation of the South Asia high. *Papers on the Tibetan Plateau Meteorological Experiment (Part II)*, Science Press, Beijing, 152–158 (in Chinese).

Sun Guowu, and Song Zhengshan, 1987: Formation of the South Asia high and its relation to circulation change and rain belt of China. *Influences of the Tibetan Plateau on the Summertime Weather in China*, Science Press, Beijing, 93–100 (in Chinese).

Tao Shiyan, and Zhu Fukang, 1964: Pattern change at 100mb and its relation to advance and retreat of the subtropical Pacific high. *Acta Meteor. Sinica*, **34**, 385–395 (in Chinese).

Zhang Jijia, and Peng Yongqing, 1983: Characteristics of the South Asia high in time and frequency. *Acta Meteor. Sinica*, **41**(3), 348–353 (in Chinese).

Zhang Qiong, Qian Yongfu, and Zhang Xuehong, 2000: Interannual and interdecadal variations of the South Asia high. *Scientia Atmospherica Sinica*, **24**(1), 67–78 (in Chinese).

Zhang Kesu, 1977: Modeling experiment of the Tibetan high and its application in summer prediction. *Scientia Sinica*, No.4, 360–368 (in Chinese).

Zhang Qiong, 1999: Laws of variation, mechanism and regional climatic effects of the South Asia high. *Ph. D. Dissertation*, Nanjing University, 148pp (in Chinese).

Zhou Jianfeng, 1991: Numerical experiments of south–north movement of the ridgeline of the South Asia high. *Acta Meteor. Sinica*, **49**(1), 96–99 (in Chinese).

Zhu Fukang, Lu Longhua, Chen Xianji, and Zhao Wei, 1980: *The South Asia high*. Science Press, Beijing, 16–17, 95 pp. (in Chinese).

南亚高压的季节变化与趋暖性

钱永甫　张　琼　姚永红　张学洪

摘　要

利用 NCEP/NCAR 再分析资料，分析了南亚高压的季节变化，讨论了对流层中高层温度、整层大气视热源和非绝热加热率的时空变化对南亚高压季节变化的影响。结果表明，南亚高压存在两个季节平衡态，即夏半年的大陆高压和冬半年的海洋高压，大陆高压又可分为青藏高压和伊朗高压。加热场对南亚高压的季节变化有重要作用，南亚高压是一个暖性高压，其中心有"趋热性"，通常位于或趋于加热率的相对大值区。南亚高压的年循环过程，主要受南亚地区潜热和感热季节变化的支配。夏季北方地区和高原地区的强烈短波辐射加热对高压中心北移和维持也有作用，长波辐射的冷却作用则是高压减弱的重要原因。

关键词：南亚高压，季节平衡态，季节变化，加热场，机制研究